Expanded View Figures

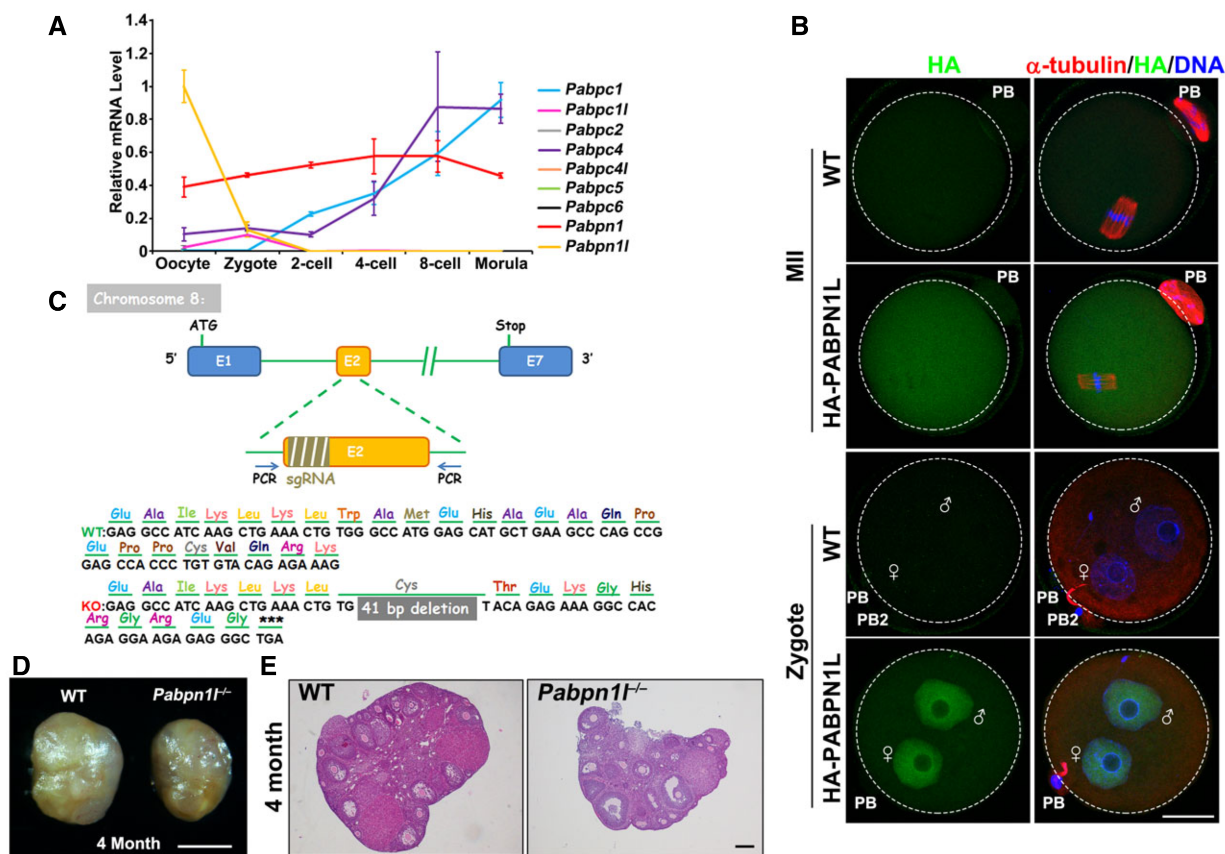

Figure EV1. *Pabpn1l* knockout in mouse and phenotype analyses.

A mRNA expression profiles of 9 PABPs detected in mouse oocytes and early embryos by RNA-seq (GSE44183). The relative mRNA level of *Pabpn1l* in oocyte was set to 1.0, and fold changes of indicated mRNAs were normalized by *Pabpn1l* (in oocyte). n = 3 biological replicates. Error bars, SEM.

B Immunofluorescent staining of HA (green) and α-tubulin (red) in WT MII oocytes and zygotes microinjected with mRNAs encoding HA-PABPN1L. DNA was labeled by DAPI. Scale bar = 20 μm.

C A strategy for CRISPR/Cas9-based mouse *Pabpn1l* knockout. Stop, stop codon; sgRNA, synthetic single-guide RNA; E1, E2, E7, exon1, 2, 7.

D Representative images of ovaries from 4-month-old WT and *Pabpn1l*$^{-/-}$ mice. Scale bar = 500 μm.

E H&E staining results showing ovarian histology of 4-month-old WT and *Pabpn1l*$^{-/-}$ mice. Scale bar = 500 μm.

© 2020 The Authors

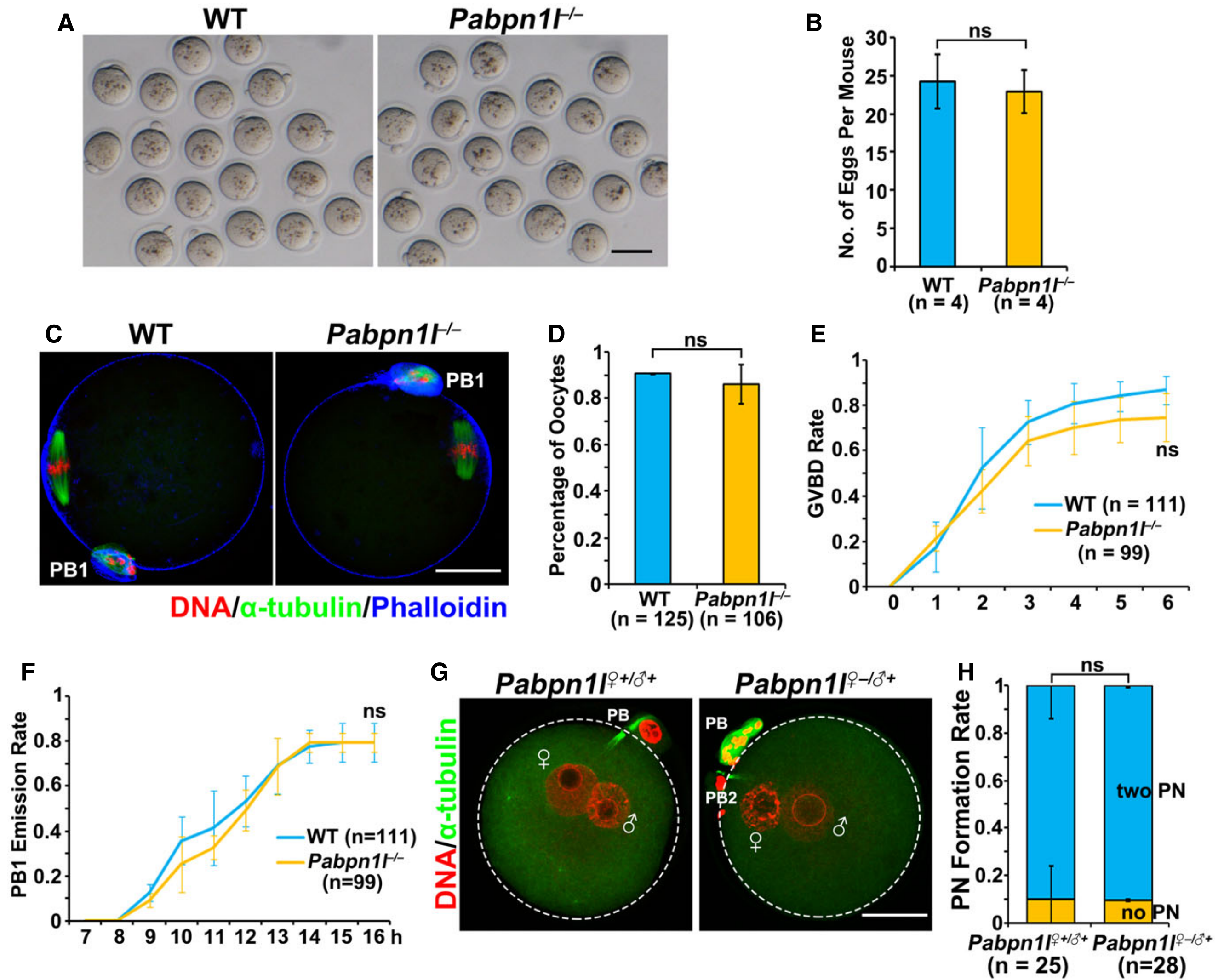

Figure EV2. Phenotype analyses of *Pabpn1l* knockout oocytes.

A Representative images of MII oocytes collected from oviducts of WT and *Pabpn1l*$^{-/-}$ mice at 16 h after hCG injection. Scale bar = 100 μm.

B Numbers of MII oocytes being ovulated by WT and *Pabpn1l*$^{-/-}$ mice (n = 4 for each genotype) after superovulation. Error bars, SEM. ns: non-significant, calculated by two-tailed Student's t-test.

C Confocal microscopy results showing spindle assembly and PB1 emission of oocytes collected from the oviducts of WT and *Pabpn1l*$^{-/-}$ mice. Scale bar = 20 μm.

D Rate of normal spindle assembly in mature WT and *Pabpn1l*$^{-/-}$oocytes.

E, F GVBD (E) and PB emission (F) rates in cultured oocytes derived from WT and *Pabpn1l*$^{-/-}$females.

G Immunofluorescent staining for α-tubulin (green) and DNA (red) in zygotes from WT and *Pabpn1l*$^{-/-}$ females 28 h after hCG injection. Scale bar = 20 μm.

H Percentage of zygotes with two pronuclei (PNs) from WT and *Pabpn1l*$^{-/-}$ females 28 h after hCG injection.

Data information: In (D, E, F, and H), the number of analyzed oocytes is indicated (n). Error bars represent SEM. ns: non-significant, calculated by two-tailed Student's t-test.

© 2020 The Authors

Figure EV3. PABPN1L interacts with BTG4.

A Immunofluorescent staining of HA (green) and DNA (red) in HeLa cells transfected with a HA-PABPN1L expressing plasmid. The white dotted box showing the PABPN1L signal was zoomed out on the right panel. Scale bar = 10 μm.

B A diagram showing of mouse BTG4 with regions of predicted disorder.

C Diagrams and co-IP results showing that BTG4 binds with PABPN1L and its N-terminal-deleted form (NterΔ). Lysates from HeLa cells expressing HA-BTG4 and FLAG-PABPN1L were immunoprecipitated with an anti-FLAG antibody. At least three independent experiments were done with consistent results.

Source data are available online for this figure.

 © 2020 The Authors

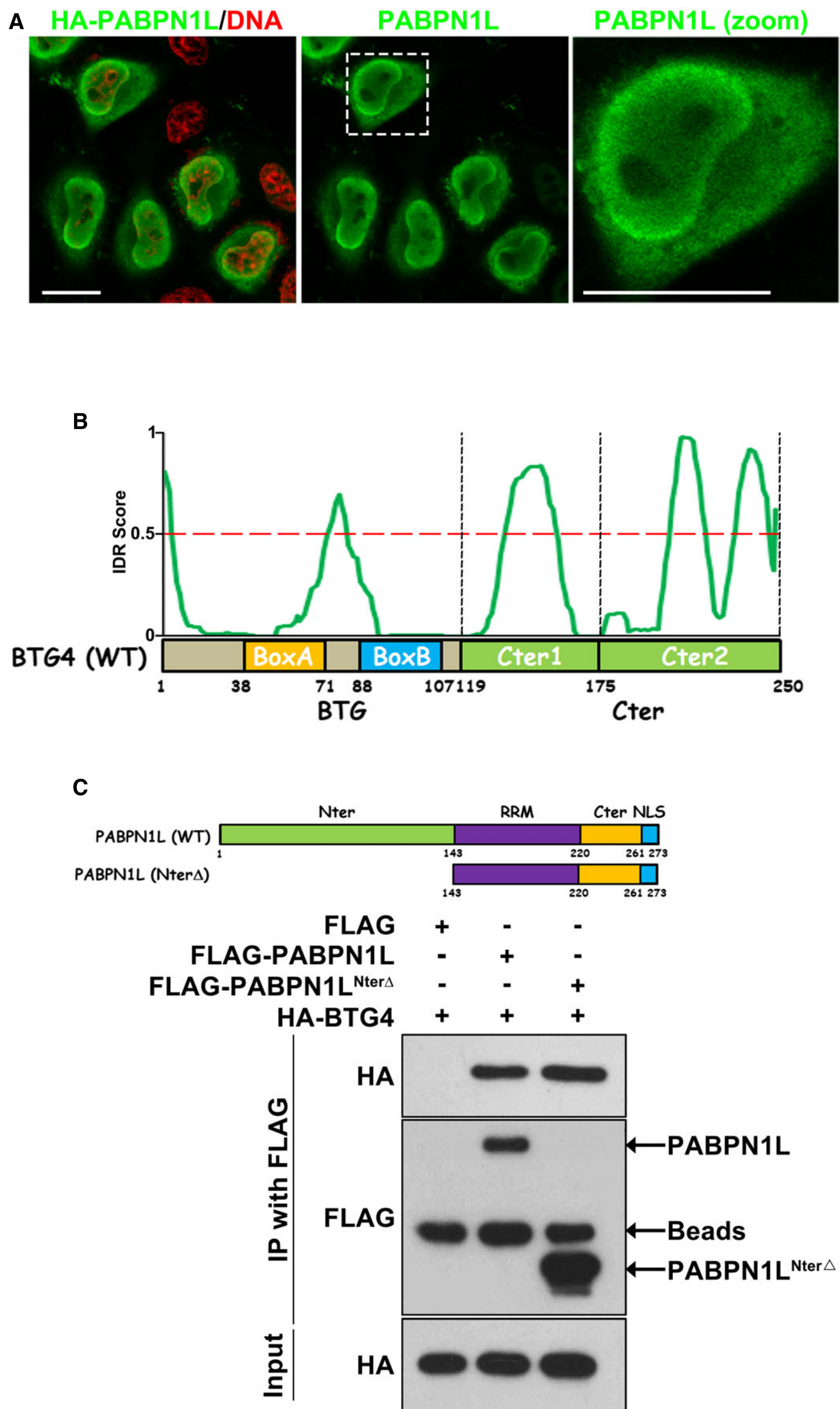

Figure EV3.

A

poly(A): protein	0	0.1	0.2	0.4	1	2
20N+A_{10}	59.61	59.38	59.34	59.27	59.25	59.23
20N+A_{20}	59.61	60.09	61.19	62.2	63.3	63.32
20N+A_{30}	57.48	58.58	59.6	60.72	61.82	61.82
20N+A_{60}	56.82	58.85	59.87	62.14	62.2	62.07
20N+A_{60} (R171A)	57.79	57.67	57.56	57.53	57.43	57.38

B

C

Figure EV4.

© 2020 The Authors

Figure EV4. Role of Arg-171 of mouse PABPN1L in RNA binding.

A A table showing the Tm in Fig 6A–C.
B Sequence alignment of mouse PABPN1L (MusPABPN1L) and *Citrus sinensis* PABPN1(CsPABPN1). The broken circle and arrowhead indicate Arg-171 of mouse PABPN1L.
C Sequence alignment and a phylogenetic tree analysis of PABPN1L. PABPN1L aminol acid sequences from *H. sapiens* (A6NDY0), *M. musculus* (Q5XFR0), *R. norvegicus* (B0BNE4), *G. gallus* (F1NWW9), *X. tropicalis* (Q28GL9), and *D. rerio* (E9QGY6) were analyzed by Clustal Omega Multiple Sequence Alignment algorithm (https://www.ebi.ac.uk/Tools/msa/clustalo/). The phylogenetic tree was plotted based on results from sequence alignments using the neighbor-joining tree algorithm without distance corrections. Sequence alignments and quality parameters of RNA recognition motif (RRM, highlighted in light yellow) and nucleus localization signal (NLS, highlighted in light blue) were generated by Jalview (http://www.jalview.org/). The broken circle and arrowhead indicate Arg-171 of mouse PABPN1L.

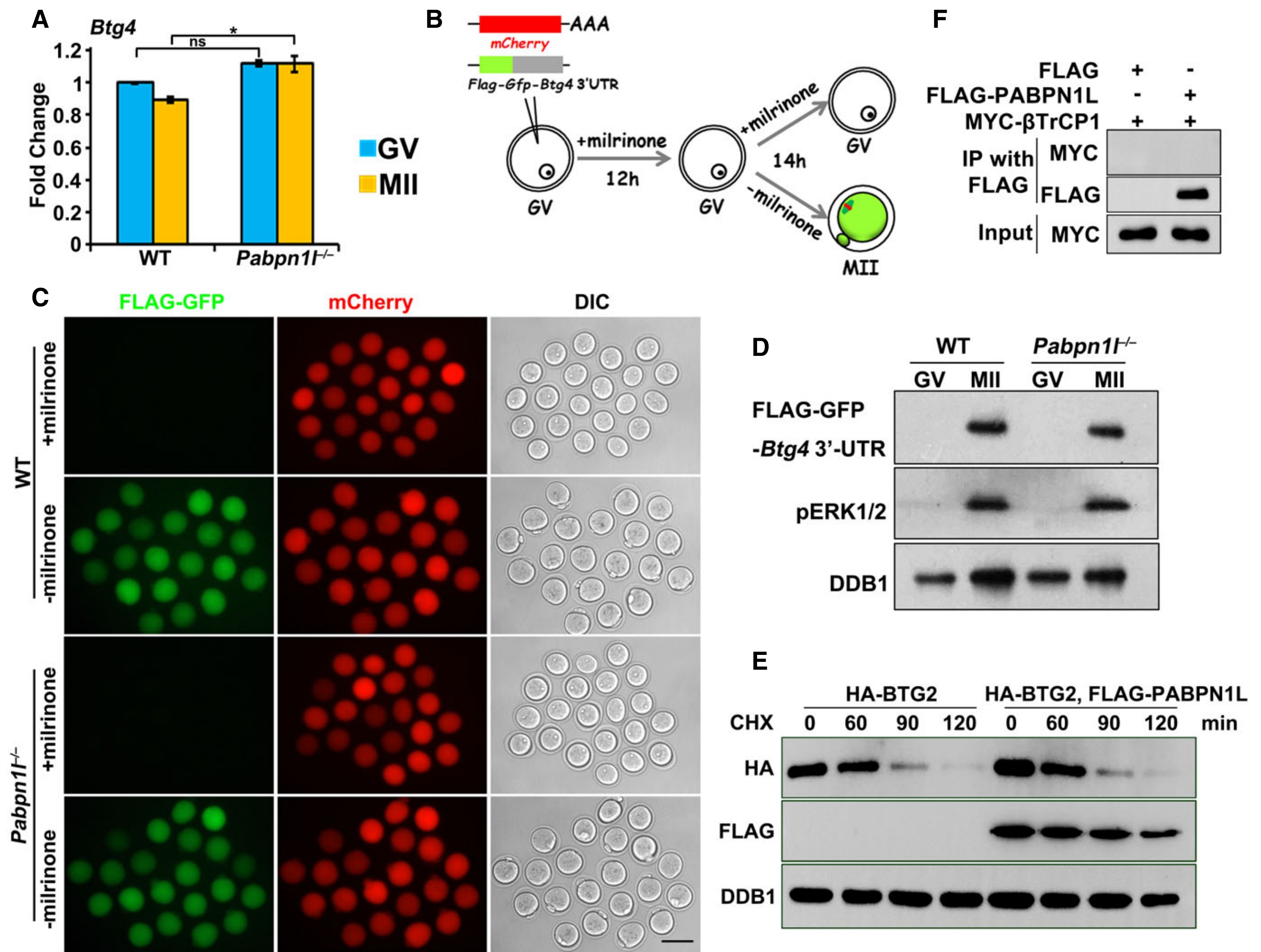

Figure EV5.

Figure EV5. Translational activity of *Btg4* 3′-UTR reporter in WT and *Pabpn1l*$^{-/-}$ oocytes.

A RT–qPCR results showing the relative levels of *Btg4* transcripts in WT and *Pabpn1l*$^{-/-}$ oocytes. n = 3 biological replicates. Error bars, SEM. *P < 0.05 by two-tailed Student's t-test. ns: non-significant.

B A diagram of the 3′-UTR reporter assay.

C Expression of FLAG-GFP fused with *Btg4* 3′-UTR in WT and *Pabpn1l*$^{-/-}$ oocytes. An *in vitro*-transcribed and polyadenylated *mCherry* mRNA was co-microinjected as a positive control. Scale bar = 100 μm.

D Western blot result showing the expression of FLAG-GFP fused with *Btg4* 3′-UTR. Total proteins from 100 oocytes were loaded in each lane. Phosphorylated ERK1/2 was blotted to indicate the developmental stages. DDB1 was blotted a loading control.

E HeLa cells were transfected with plasmids expressing HA-BTG2 and FLAG-PABPN1L for 12 h and then treated by CHX (10 μM). Cells were harvested at the indicated time points for Western blot analysis.

F Co-IP and Western blot results showing that βTrCP1 did not interact with PABPN1L. Lysates from HeLa cells expressing MYC-βTrCP1 and FLAG-PABPN1L were immunoprecipitated with an anti-FLAG antibody.

Data information: For all Western blot results, at least three independent experiments were done with consistent results.

Source data are available online for this figure.

© 2020 The Authors